

Original article

1  
2  
3 **Functional lung avoidance in radiotherapy using optimisation of**  
4 **biologically effective dose with non-coplanar beam orientations**

5  
6 James L Bedford and Merina Ahmed

7  
8 The Institute of Cancer Research and The Royal Marsden NHS Foundation Trust, London,  
9 UK

10  
11 **Corresponding Author:**

12 James Bedford, Joint Department of Physics, The Institute of Cancer Research and The Royal  
13 Marsden NHS Foundation Trust, Downs Road, Sutton, London, SM2 5PT, UK.

14 James.Bedford@icr.ac.uk

15  
16 **Running title:** Functional lung avoidance

17  
18 **Funding:** National Institute for Health Research (NIHR) Biomedical Research Centre at the  
19 Royal Marsden NHS Foundation Trust and the Institute of Cancer Research.

20 Cancer Research UK under Program No. C33589/A19727.

21 Cancer Research UK Centres Network Accelerator Award Grant (A21993) to the ART-NET  
22 consortium.

23  
24 **Abstract word count:** 248

25 **Main text word count:** 2970

26

## 27 **Background and Purpose**

28 In external beam radiotherapy for non-small cell lung cancer, dose to functioning lung should  
29 be minimised to reduce lung morbidity. This study aimed to develop a method for avoiding  
30 beam delivery through functional lung and to quantify the possible benefit to the patients.

31

## 32 **Materials and Methods**

33 Twelve patients that were treated as part of a clinical trial of single photon emission  
34 computed tomography (SPECT) functional lung avoidance were retrospectively studied.  
35 During treatment planning, the dose in the lung was weighted by the relative intensity of the  
36 functional image. A single conformal beam was scanned systematically around the planning  
37 target volume to find optimum orientations and the resulting map of functional dose variation  
38 with gantry and couch angle was used to select five non-coplanar intensity-modulated beams,  
39 taking into account directions prohibited due to collision risk. Expected reduction in  
40 pneumonitis risk was calculated using a logistic model.

41

## 42 **Results**

43 The volume of lung irradiated to a functionally weighted dose of 5Gy was 11.8% (range  
44 3.5%-22.0%) for functional plans, versus 20.9% (range 4.9%-33.3%) for conventional  
45 VMAT plans ( $p=0.002$ ). Mean functionally weighted dose was 4.1Gy (range 1.3Gy-7.2Gy)  
46 for functional plans, versus 4.5Gy (range 1.5Gy-8.3Gy) for conventional plans ( $p=0.002$ ).  
47 Predicted pneumonitis risk was reduced by 4.3% (range 0.4%-15.6%) ( $p=0.002$ ).

48

## 49 **Conclusions**

50 By seeking the optimum non-coplanar beam orientations, it is possible to reduce dosimetric  
51 lung parameters by 10% or more, consistently in all patients, regardless of the pattern of lung  
52 perfusion. A prediction model indicates that this will improve radiation-associated lung  
53 injury.

54

## 55 **MeSH Keywords**

56 Carcinoma, Non-Small-Cell Lung

57 Retrospective Studies

58 Radiation Injuries

59 Tomography, Emission-Computed, Single-Photon

60 Perfusion

## 61 **1. Introduction**

62 Over the last two decades, a number of studies have been conducted to incorporate lung  
63 function information into treatment planning of non-small cell lung cancer [1-2]. The  
64 concept is to use a radiolabelled tracer in conjunction with a single photon emission  
65 computed tomography (SPECT) scan to define the perfused regions of the lung and this  
66 information is used in tandem with a planning computed tomography (CT) scan for treatment  
67 planning. The radiotherapy is delivered through the regions with poorer function, thereby  
68 leaving the more perfused or ventilated regions relatively undamaged, with the aim that the  
69 patients are less likely to suffer from radiation pneumonitis [3-8]. A recent review therefore  
70 concludes that use of SPECT information for functional lung avoidance is valuable, although  
71 definite dose constraints for practical planning are deficient [9].

72

73 However, the clinical results have so far been disappointing [10], which may be due  
74 to several reasons. Firstly, definition of normally functioning lung is variable from study to  
75 study, as the threshold in the functional image is undecided. Typically, the threshold at  
76 which the lung is taken to be functioning is 30% of the maximum SPECT signal, but there is  
77 no firm basis for this [11]. Secondly, directing radiation beams through regions of poor  
78 function is difficult in many patients due to the pattern of perfusion. If the perfusion deficits  
79 are broadly spread over the lung volume, it is difficult to direct beams through these regions  
80 [12-13]. Thirdly, it is unclear how much sparing of functioning lung is necessary to produce  
81 a measurable clinical benefit.

82

83 This paper aims to address these difficulties. By using dose distributions weighted by  
84 the lung function, the need for a threshold in function is avoided. Most importantly, this  
85 study presents a method of selecting those non-coplanar beam orientations which direct  
86 radiation through the least functional parts of the lung, so that the benefit of functional lung  
87 avoidance is maximised. Finally, the relationship between mean lung dose and clinical rate  
88 of pneumonitis is used to investigate the expected clinical benefit resulting from the  
89 dosimetric lung sparing obtained.

90

## 91 **2. Materials and Methods**

### 92 *2.1. Patients and scans*

93 In this study, 12 patients from a clinical trial aiming to correlate irradiated volumes of  
94 anatomic and functional lung with radiation induced lung damage [11] were examined

95 retrospectively. The clinical trial itself was performed in accordance with the ethical  
96 standards of the institutional and/or national research committee and with the 1964  
97 Helsinki declaration and its later amendments or comparable ethical standards. Written  
98 informed consent was obtained from all individual participants included in the study.  
99

100 For radiotherapy treatment planning, the patients were CT scanned in breath-hold  
101 using an Active Breathing Coordinator (ABC) device (Elekta AB, Stockholm, Sweden) [14]  
102 and then SPECT scanned within four hours using 200 MBq of  $^{99m}\text{Tc}$ -radiolabelled  
103 macroalbumin aggregate (MAA), to determine lung function. Further details of the scanning  
104 protocol are given elsewhere [11]. The functional scans were rigidly registered with the CT  
105 scans using a series of surface markers which contained radiotracer for the SPECT scans and  
106 were also visible on the CT scans. Use of ABC for the planning CT scan, so as to optimise  
107 the quality of treatment plan, but free breathing for the SPECT scan, in view of the time taken  
108 to acquire the scan, resulted in poor image matching around the diaphragm, but none of the  
109 target volumes in this study were located in this area, so this was not considered to be an  
110 issue. Gross tumour volume (GTV) was delineated on the CT scans and an isotropic margin  
111 of 5 mm was added to define the clinical target volume (CTV). A further margin of 5 mm  
112 was then added to the CTV to create the planning target volume (PTV). For two patients  
113 treated without ABC, the PTV margin was 5 mm laterally and 10 mm superiorly and  
114 inferiorly.  
115

115

## 116 *2.2. Treatment planning*

117 In this retrospective study, AutoBeam v6.1 [15-16] was used to create functional inverse  
118 plans. The SPECT scans were renormalised to the maximum intensity value in the scan and  
119 the dose to the lung region was then weighted by the corresponding relative function [17].  
120 To ensure that the PTV dose distribution was not affected by this process, the PTV plus a  
121 margin of 5 mm was excluded from the lung region with functional weighting. As the  
122 functional weighting was a continuous variable, it was not necessary to define thresholds for  
123 function. However, for purposes of comparison with other studies, the lung volumes with  
124 greater than 25% function ( $\text{FL}_{25\%}$ ) and 50% function ( $\text{FL}_{50\%}$ ) were delineated by  
125 thresholding.  
126

126

127 Treatment planning was conducted using a beam model for the 6 MV beam of a Versa  
128 HD accelerator (Elekta AB, Stockholm, Sweden) [18]. To define the optimum beam

129 orientations for delivery of functionally weighted dose, a single conformal beam was scanned  
130 systematically through all gantry angles from  $180^\circ$  on one side of the couch to  $180^\circ$  on the  
131 other side of the couch and, for each of these gantry angles, the beam was scanned from  
132 couch angle  $270^\circ$  to  $90^\circ$ , giving a grid of gantry/couch combinations. The beam was  
133 normalised so that the mean PTV dose was 1.0. The mean functionally weighted lung dose  
134 resulting from each beam orientation was then plotted. Orientations not feasible due to  
135 collisions of gantry and couch were then omitted.

136

137 Complete treatment plans were then constructed consisting of five static intensity-  
138 modulated radiation therapy (IMRT) beams, each containing 10 segments. The directions of  
139 these beams were manually chosen based on the maps of mean functionally weighted lung  
140 dose as a function of beam orientation. Generally, the orientations that minimised the  
141 functionally weighted mean lung dose were selected, but in some cases, it was necessary to  
142 choose orientations with higher lung dose in order to ensure homogeneous PTV coverage and  
143 conformal distribution of dose around the PTV. Final plans were calculated using a  
144 convolution algorithm [19-20] on a dose grid of  $2.5\text{mm}\times 2.5\text{mm}\times 2.5\text{mm}$ .

145

146 For comparison, a standard treatment plan was constructed for each patient, consisting  
147 of a single anticlockwise volumetric modulated arc therapy (VMAT) arc from  $179^\circ$  to  $181^\circ$   
148 gantry angle, with control points at  $2^\circ$  intervals. Similar to current clinical practice at this  
149 centre, the arcs were designed to be mostly conformally shaped so as to provide robust  
150 dosimetry in the event of tumour shrinkage during the course of treatment [21]. Functional  
151 dose weighting was initially turned off, so that the plan was based on physical lung dose.  
152 After optimisation, the functional weighting was applied for lung so that the plan could be  
153 compared with the functional treatment plan. To understand the potential bias of using IMRT  
154 for the functional treatment plans and VMAT for the comparison plans, a coplanar IMRT  
155 plan with five equally spaced beams was created, each beam having 10 segments per beam.  
156 As with the VMAT plan, optimisation was performed without function and then functional  
157 weighting was applied at the end.

158

### 159 *2.3. Prediction of outcome*

160 The expected clinical benefit of the functional planning approach was evaluated by  
161 calculating predicted radiation pneumonitis risk using the logistic model and fitting  
162 parameters described by QUANTEC [22]. For each patient and type of plan, the mean

163 functionally weighted dose,  $D_f$ , was applied to the formula so as to reflect the benefit of the  
 164 biological optimisation. However, the process of calculating  $D_f$  for each patient by weighting  
 165 the physical dose by function and then taking the mean had the effect of rescaling the dose.  
 166 On average, over the entire group of patients, this rescale factor was the mean relative  
 167 function of the population,  $k$ . To remove the rescaling for application to the QUANTEC  
 168 formula, the mean functional dose of each patient and plan was therefore divided by  $k$ . Then  
 169 the probability of radiation pneumonitis,  $p$ , was given by:

$$171 \quad p = \frac{\exp(b_0 + b_1 D_f / k)}{1 + \exp(b_0 + b_1 D_f / k)}. \quad (1)$$

172  
 173 The fitting parameters were those given by Marks et al. [22]:  $b_0 = -3.87$  and  $b_1 = 0.126 \text{Gy}^{-1}$ .  
 174 The value of  $k$  was estimated as part of the study.

175  
 176 The functional and standard plans were compared in SPSS v29 (IBM Corp., Armonk,  
 177 NY) using two-tailed Wilcoxon matched pair signed-rank tests, with a null hypothesis that  
 178 the statistics for the two types of plan were from the same distribution.

### 179 180 **3. Results**

#### 181 *3.1. Lung perfusion*

182 Patterns of lung perfusion varied widely between patients. Some patients had moderate  
 183 perfusion over the entire lung volume, whereas other patients had patches of well-perfused  
 184 lung separated by regions of poor perfusion. Figure 1 shows examples of each type of  
 185 perfusion. After normalisation of the lung function, the mean function in the lung volume  
 186 was found to vary among the patients from 0.18 to 0.38, with a median over the 12 patients of  
 187 0.24. Thus, the value of the function factor  $k$  in equation (1) was taken to be 0.24.

#### 188 189 *3.2. Beam orientation maps*

190 The beam orientation maps for the patients of figure 1 are shown in figure 2. Use of lateral  
 191 beams generally gave a high mean functional dose as the beams traversed both lungs at their  
 192 broadest dimension. Furthermore, with a large PTV, the beam aperture was larger, and  
 193 consequently the mean lung dose was higher for all beam positions. For homogeneous  
 194 perfusion, it was relatively difficult to find minima in which to place beams, but for

195 inhomogeneous perfusion, there were several options available, in which case the greatest  
196 spread of beams was chosen so as to increase conformality.

197

### 198 3.3. Dose statistics

199 Figure 3 shows mean dose-volume histograms for the functional and conventional plans. At  
200 functional doses above 20Gy, there was no difference between the functional and standard  
201 plans because these higher doses related to the region immediately around the PTV, where it  
202 was not possible to minimise lung dose without compromising PTV coverage, and where  
203 functional weighting was also not applied. There was some lung sparing in the range of  
204 functionally weighted doses from 0 to 20Gy. Note that with the median function being 0.24, a  
205 physical dose of 20Gy equated to a functionally weighted dose of 5Gy, where the difference  
206 between functional and conventional plans was greatest. The sparing of the thresholded  
207 FL<sub>25%</sub> and FL<sub>50%</sub> regions was shown to be considerable at doses of 0 to 20Gy, again with  
208 maximum effect around 5Gy, which was likely to be clinically important. Dose-volume  
209 histograms for the lung volumes with the coplanar IMRT plan are also shown in figure 3a and  
210 3b. There was a small improvement in irradiated volume of lung with the IMRT plan  
211 compared to VMAT, but this did not detract from the obvious benefit of the non-coplanar  
212 functional plan.

213

214 The statistics for the PTV and lung are shown for all of the patients individually in  
215 figure 4. The PTV homogeneity was generally better in the functionally weighted plans  
216 ( $p=0.003$ ), although this was unlikely to be clinically significant (figure 4a). The  $V_{5Gy}$  for the  
217 weighted lung dose was lower for the optimised plans ( $p=0.002$ ) (figure 4b). Similarly, mean  
218 functionally weighted lung dose was lower for all cases when using the orientation-optimised  
219 plans ( $p=0.002$ ) (figure 4c). In the well-functioning lung as defined by FL<sub>50%</sub>, there was also  
220 a lower functionally weighted  $V_{20Gy}$  ( $p=0.03$ ) (figure 4d).

221

222 The statistics for all of the structures are shown in figure 5. Mean heart dose was  
223 slightly higher with the optimised plans (median 6.5Gy; range 0.1Gy to 31.2Gy), than with  
224 coplanar plans (median 2.1Gy; range 0.0Gy to 22.8Gy) due to the beams avoiding the lungs  
225 ( $p=0.01$ ). Mean dose to the oesophagus with the optimised plans (median 14.5Gy, range  
226 5.3Gy to 35.6Gy) was lower than with the standard coplanar plans (median 17.4Gy, range  
227 6.5Gy to 36.8Gy,  $p=0.02$ ). The spinal cord planning risk volume was similar between the  
228 two techniques ( $p=0.1$ ).

229

230 *3.4. Prediction of outcome*

231 The predicted radiation pneumonitis risk for the conventional and functional plans is  
232 shown in figure 6. The largest reductions in risk were seen in the patients with the highest  
233 initial risk, due to the increased steepness of the logistic model with increasing dose.  
234 However, some benefit was predicted for all patients. Overall, the median reduction in risk  
235 was 4.3% (range 0.4% to 15.6%) ( $p=0.002$ ).

236

237 **4. Discussion**

238 In external beam radiotherapy for non-small cell lung cancer, dose to functioning lung should  
239 be minimised to reduce lung morbidity. This study weights the dose in lung by the relative  
240 function and then selects beam orientations to minimise that weighted lung dose, resulting in  
241 a reduction in irradiated volume from 21% to 12%, with a reduction in functionally weighted  
242 mean lung dose from 4.5Gy to 4.1Gy. This is predicted to reduce pneumonitis by  
243 approximately 4%.

244

245 The study therefore supports the view of De Bari et al. [9] that use of SPECT to define  
246 functioning lung is a valuable asset in the treatment of non-small cell lung cancer. However,  
247 the production of treatment plans which significantly spare normal lung is found to require  
248 substantial application of functionally-weighted treatment planning and non-coplanar beam  
249 orientations. The use of functionally weighted dose enables the continuous spectrum of  
250 function values to be used, without having to make arbitrary decisions concerning the  
251 threshold level of function at which the lung is taken to be functioning normally [1, 3, 23-24].  
252 This type of weighting is very simple to apply, although such an option is not currently  
253 available in many treatment planning systems, so widespread implementation would require  
254 input from the vendors. The limitation of using ABC for the planning CT scan and free  
255 breathing for the SPECT could be resolved in a future study by the use of deformable image  
256 registration to adapt the SPECT scan to the contour of the breath-hold planning scan.

257

258 The use of non-coplanar beams, although not as streamlined practically as a single  
259 VMAT arc, is necessary to maximise the avoidance of functioning lung, and in today's  
260 complex treatment environment, is actually a relatively simple technique. Several non-  
261 coplanar VMAT arcs could be used in place of the fixed IMRT beams, but as the IMRT  
262 beams are directed very specifically at the minima of the beam orientation maps, it is



263 expected that spreading out the orientations over VMAT arc lengths would reduce the value  
264 of the solution, so is not presently recommended. Adding an automated selection algorithm  
265 to the present study is expected to increase the convenience of the beam selection in the event  
266 of clinical application, but it is not expected to improve the dosimetric or clinical benefit of  
267 the technique.

268

269 Taking the functional weighting factor,  $k$  (equation 1) to be approximately 0.24, the  
270 observed reduction in functional mean lung dose corresponds to a conventional physical  
271 mean dose of 18Gy, reduced to 16Gy. Similarly, with functional  $V_{5Gy}$ , which approximately  
272 translates to  $V_{20Gy}$  in conventional physical absorbed dose, the value can be reduced by 40%  
273 of its initial value. These benefits in functional lung dose are similar those reported  
274 previously, although the deliverability of some of the previous techniques is unclear [24, 25].  
275 Both mean lung dose and irradiated volume are in some way related to the clinical incidence  
276 of radiation pneumonitis [22, 26-27] and dosimetric statistics of the functioning subvolumes  
277 of lung are also known to be correlated with post-radiotherapy lung function outcomes [11,  
278 28]. With these results, it is expected that a clinical trial similar to that reported by Yaremko  
279 et al [10] would report a benefit for functional lung avoidance. Vinogradskiy et al. [29] and  
280 Miller et al. [30] report positive results in a phase II non-randomised trial against historical  
281 controls for patients selected according to considerable functional deficits around the PTV.  
282 The dosimetric benefits of the present study would enable trials such as these to be opened to  
283 a wider spectrum of patients. Note, however, that some of these reported studies are based on  
284 ventilation rather than perfusion and the relationship between the two varies considerably  
285 [31]. Both ventilation and perfusion should be correlated for lung function to be effective  
286 [32], so it is possible that both of these should be included in clinical studies [33].

287

288 Some of the studies in the literature show an increase in PTV dose inhomogeneity and  
289 an increase in heart dose, due to the redistribution of beams through the mediastinum to avoid  
290 functioning lung [7, 24]. In the present study, no attempt is made to force the critical  
291 structures to receive equal dose, so the change of beam orientations has a noticeable effect on  
292 the organs at risk, including the heart. The increase in mean heart dose from 2.1Gy to 6.5Gy  
293 may be of relevance for long term cardiac morbidity, but 6.5Gy is still substantially lower  
294 than the 10Gy reported by Vinogradskiy et al. [29] and the 13Gy reported by Yaremko et al.  
295 [10]. It is also much lower than the constraint of median dose less than 25Gy suggested by  
296 Khalil et al. [34] in a proposed study protocol. A possible means of avoiding a higher heart

297 dose is to add the mean heart dose to the mean functional lung dose when creating the beam  
298 orientation maps, or to generalise the method further to include all organs at risk with  
299 contributions weighted by importance factors, so that the beam orientation maps represent  
300 objective function maps [35]. The entire beam selection method may also be used for  
301 avoidance of other parallel organs.

302

303         The pneumonitis risk model calculated that the reduction in dose to functioning lung  
304 demonstrated in this study should translate into a clinical reduction of pneumonitis by around  
305 4%, although in some patients with high initial lung doses due to large PTV, the reduction in  
306 risk of lung damage was as much as 20%. The greatest benefit was expected to be observed  
307 in patients with unevenly perfused lungs and in patients having focal mismatch defects. The  
308 value of the method was also expected to be maximal for patients with previous lung surgery  
309 where dose could be delivered towards peri-operative cavities and in patients with upper lobe  
310 tumours where better cardiac sparing could be achieved. However, the clinical performance  
311 of the technique could ultimately only be quantified by a well-controlled clinical trial.

312

313

**314 Acknowledgments**

315 The authors acknowledge funding from the National Institute for Health Research (NIHR)  
316 Biomedical Research Centre at the Royal Marsden NHS Foundation Trust and the Institute of  
317 Cancer Research. The views expressed are those of the authors and not necessarily those of  
318 the NHS, the NIHR or the Department of Health. This work has also been supported by  
319 Cancer Research UK under Program No. C33589/A19727, and by a Cancer Research UK  
320 Centres Network Accelerator Award Grant (A21993) to the ART-NET consortium. The  
321 authors also thank those who contributed to the clinical trial prior to this study: Dr Alex  
322 Weller, Dr Alex Dunlop, Adam Oxe, Ranga Gunapala, Dr Iain Murray, Matthew J Gray, Dr  
323 Glenn D Flux, and Professor Nandita M deSouza. The authors are also grateful for the  
324 support of Professor Uwe Oelfke and Dr Michael Thomas.

325

326 **References**

- 327 [1] Seppenwoolde Y, Engelsman M, De Jaeger K, Muller SH, Baas P, McShan DL, et al.  
328 Optimizing radiation treatment plans for lung cancer using lung perfusion  
329 information. *Radiother Oncol* 2002;63:165-77.
- 330 [2] Christian JA, Partridge M, Nioutsikou E, Cook G, McNair HA, Cronin B, et al. The  
331 incorporation of SPECT functional lung imaging into inverse radiotherapy planning  
332 for non-small cell lung cancer. *Radiother Oncol* 2005;77:271-7.
- 333 [3] Marks LB, Sherouse GW, Munley MT, Bentel GC, Spencer DP. Incorporation of  
334 functional status into dose-volume analysis. *Med Phys* 1999;26:196-9.
- 335 [4] McGuire SM, Zhou S, Marks LB, Dewhurst M, Yin F-F, Das SK. A methodology for  
336 using SPECT to reduce intensity-modulated radiation therapy (IMRT) dose to  
337 functioning lung. *Int J Radiat Oncol Biol Phys* 2006;66:1543–52.
- 338 [5] Farr KP, West K, Yeghiaian-Alvandia R, Farlow D, Stensmyr R, Chicco A, et al.  
339 Functional perfusion image guided radiation treatment planning for locally advanced  
340 lung cancer. *Phys Imaging Radiat Oncol* 2019;11:76-81.
- 341 [6] Waxweiler T, Schubert L, Diot Q, Faught A, Stuhr K, Castillo R, et al. A complete  
342 4DCT-ventilation functional avoidance virtual trial: Developing strategies for  
343 prospective clinical trials. *J Appl Clin Med Phys* 2017;18:144-52.
- 344 [7] Lee E, Zeng J, Miyaoka RS, Saini J, Kinahan PE, Sandison GA, et al. Functional  
345 lung avoidance and response-adaptive escalation (FLARE) RT: Multimodality plan  
346 dosimetry of a precision radiation oncology strategy. *Med Phys* 2017;44:3418-29.
- 347 [8] Seyedin SN, Bassalow R, Mawlawi OR, Turner LM, Patel RR, Mazin SR, et al. The  
348 potential of biology-guided radiation therapy in thoracic cancer: A preliminary  
349 treatment planning study. *Front Oncol* 2022;12:921473.
- 350 [9] De Bari B, Deantonio L, Bourhis J, Prior JO, Ozsahin M. Should we include SPECT  
351 lung perfusion in radiotherapy treatment plans of thoracic targets? Evidences from the  
352 literature. *Critical Reviews in Oncology/Hematology* 2016;102:111-7.
- 353 [10] Yaremko BP, Capaldi DPI, Sheikh K, Palma DA, Warner A, Dar AR, et al.  
354 Functional lung avoidance for individualized radiation therapy: results of a double-  
355 masked, randomized controlled trial. *Int J Radiation Oncol Biol Phys* 2022;113:1072-  
356 84.
- 357 [11] Weller A, Dunlop A, Oxeer A, Gunapala R, Murray I, Gray MJ, et al. Spect perfusion  
358 imaging versus CT for predicting radiation injury to normal lung in lung cancer  
359 patients. *Br J Radiol* 2019;92:20190184.

- 360 [12] Lavrenkov K, Christian JA, Partridge M, Niotsikou E, Cook G, Parker M, et al. A  
361 potential to reduce pulmonary toxicity: The use of perfusion SPECT with IMRT for  
362 functional lung avoidance in radiotherapy of non-small cell lung cancer. *Radiother  
363 Oncol* 2007;83:156-62.
- 364 [13] Lavrenkov K, Singh S, Christian JA, Partridge M, Nioutsikou E, Cook G, et al.  
365 Effective avoidance of a functional spect-perfused lung using intensity modulated  
366 radiotherapy (IMRT) for non-small cell lung cancer (NSCLC): An update of a  
367 planning study. *Radiother Oncol* 2009;91:349-52.
- 368 [14] Panakis N, McNair HA, Christian JA, Mendes R, Symonds-Taylor JRN, Knowles C,  
369 et al. Defining the margins in the radical radiotherapy of non-small cell lung cancer  
370 (NSCLC) with active breathing control (ABC) and the effect on physical lung  
371 parameters. *Radiother Oncol* 2008;87:65-73.
- 372 [15] Bedford JL. Treatment planning for volumetric modulated arc therapy. *Med Phys*  
373 2009;36:5128-38.
- 374 [16] Bedford JL. Sinogram analysis of aperture optimization by iterative least-squares in  
375 volumetric modulated arc therapy. *Phys Med Biol* 2013;58:1235-50.
- 376 [17] Nioutsikou E, Partridge M, Bedford JL, Webb S. Prediction of radiation-induced  
377 normal tissue complications in radiotherapy using functional image data. *Phys Med  
378 Biol* 2005;50:1035-46.
- 379 [18] Bedford JL, Thomas MDR, Smyth G. Beam modeling and VMAT performance with  
380 the Agility 160-leaf multileaf collimator. *J Appl Clin Med Phys* 2013;14:172-85.
- 381 [19] Bedford JL. Speed versus accuracy in a fast convolution photon dose calculation for  
382 conformal radiotherapy. *Phys Med Biol* 2002;47:3475-84.
- 383 [20] Bedford JL, Nilawar R, Nill S, Oelfke U. A phase space model of a Versa HD linear  
384 accelerator for application to Monte Carlo dose calculation in a real-time adaptive  
385 workflow. *J Appl Clin Med Phys* 2022;23:e13663.
- 386 [21] Bedford JL, Hansen VN, McNair HA, Aitken AH, Brock JEC, Warrington AP, et al.  
387 Treatment of lung cancer using volumetric modulated arc therapy and image  
388 guidance: A case study. *Acta Oncol* 2008;47:1438-43.
- 389 [22] Marks LB, Bentzen SM, Deasy JO, Kong F-M, Bradley JD, Vogelius IS, et al.  
390 Radiation dose–volume effects in the lung. *Int J Radiat Oncol Biol Phys*  
391 2010;76:S70-6.

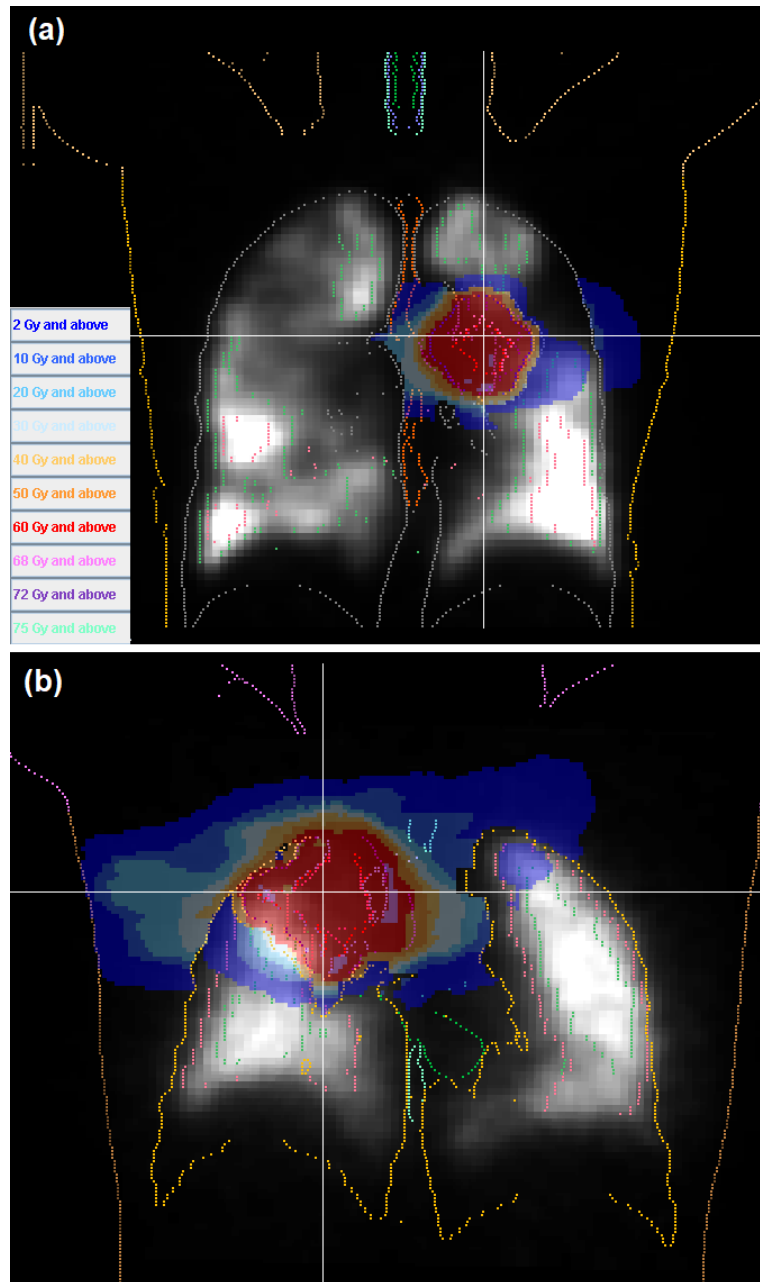
- 392 [23] Miften MM, Das SK, Su M, Marks LB. Incorporation of functional imaging data in  
393 the evaluation of dose distributions using the generalized concept of equivalent  
394 uniform dose. *Phys Med Biol* 2004;49:1711-21.
- 395 [24] Matuszak MM, Matrosic C, Jarema D, McShan DL, Stenmark MH, Owen D, et al.  
396 Priority-driven plan optimization in locally advanced lung patients based on perfusion  
397 SPECT imaging. *Adv Radiat Oncol* 2016;1:281-9.
- 398 [25] McGuire SM, Marks LB, Yin FF, Das SK. A methodology for selecting the beam  
399 arrangement to reduce the intensity-modulated radiation therapy (IMRT) dose to the  
400 SPECT-defined functioning lung. *Phys Med Biol* 2010;55:403-16.
- 401 [26] Kwa SIS, Lebesque JV, Theuws JCM, Marks LB, Munley MT, Bentel G, et al.  
402 Radiation pneumonitis as a function of mean lung dose: An analysis of pooled data of  
403 540 patients. *Int J Radiat Oncol Biol Phys* 1998;42:1-9.
- 404 [27] Yorke ED, Jackson A, Rosenzweig KE, Braban L, Leibel SA, Ling CC. Correlation  
405 of dosimetric factors and radiation pneumonitis for non-small-cell lung cancer  
406 patients in a recently completed dose escalation study. *Int J Radiat Oncol Biol Phys*  
407 2005;63:672-82.
- 408 [28] Ghassemi N, Castillo R, Castillo E, Jones BL, Miften M, Kavanagh B, et al.  
409 Evaluation of variables predicting PFT changes for lung cancer patients treated on a  
410 prospective 4DCT-ventilation functional avoidance clinical trial. *Radiother Oncol*  
411 2023;187:109821.
- 412 [29] Vinogradskiy Y, Castillo R, Castillo E, Schubert L, Jones BL, Faught A, et al.  
413 Results of a multi-institutional phase 2 clinical trial for 4DCT-ventilation functional  
414 avoidance thoracic radiation therapy. *Int J Radiat Oncol Biol Phys* 2022;112:986-95.
- 415 [30] Miller R, Castillo R, Castillo E, Jones BL, Miften M, Kavanagh B, et al.  
416 Characterizing pulmonary function test changes for patients with lung cancer treated  
417 on a 2-institution, 4-dimensional computed tomography-ventilation functional  
418 avoidance prospective clinical trial. *Adv Radiat Oncol* 2023;8:101133.
- 419 [31] Li Z, Le Roux P-Y, Callahan J, Hardcastle N, Hofman M S, Siva S, et al.  
420 Quantitative assessment of ventilation-perfusion relationships with gallium-68  
421 positron emission tomography/computed tomography imaging in lung cancer patients.  
422 *Phys Imaging Radiat Oncol* 2022;22:8-12.
- 423 [32] Petersson J, Glenny RW. Gas exchange and ventilation–perfusion relationships in the  
424 lung. *Eur Respir J* 2014;44:1023-41.

- 425 [33] Nakajima Y, Kadoya N, Kimura T, Hioki K, Jingu K, Yamamoto T. Variations  
426 between dose-ventilation and dose-perfusion metrics in radiation therapy planning for  
427 lung cancer. *Adv Radiat Oncol* 2020;5:459-65.
- 428 [34] Khalil AA, Hau E, GebSKI V, Grau C, Gee H, Nyeng TB, et al. Personal innovative  
429 approach in radiation therapy of lung cancer-functional lung avoidance SPECT-  
430 guided (ASPECT) radiation therapy: a study protocol for phase II randomised double-  
431 blind clinical trial. *BMC Cancer* 2021;21:940.
- 432 [35] Smyth G, Bamber JC, Evans PM, Bedford JL. Trajectory optimization for dynamic  
433 couch rotation during volumetric modulated arc radiotherapy. *Phys Med Biol*  
434 2013;58:8163-77.

435 **Figures**

436

437



438

439

440

441 Figure 1. Coronal view of two patients, showing the relative lung perfusion. Patient

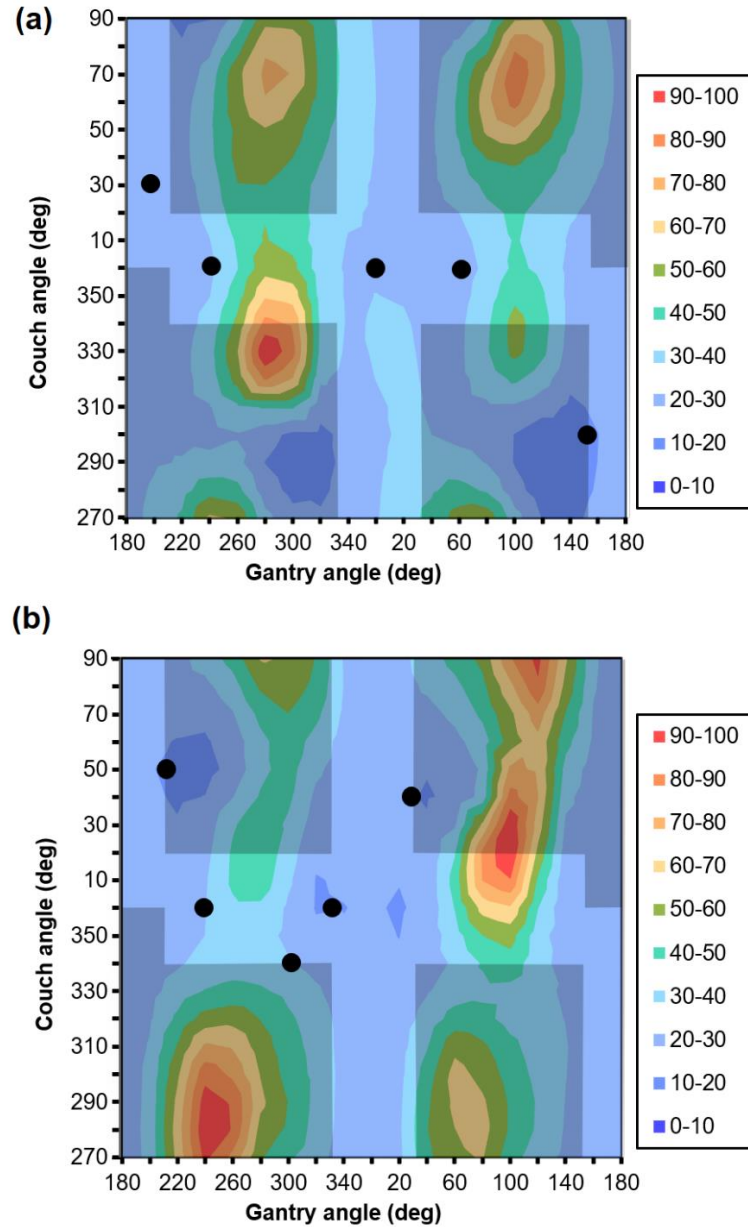
442 (a) has variable perfusion, and patient (b) has more uniform perfusion. The dose distribution

443 resulting from the functional non-coplanar treatment plan is shown in colour, with the colour

444 key in the bottom left of (a).

445





446

447

448

449

450

451

452

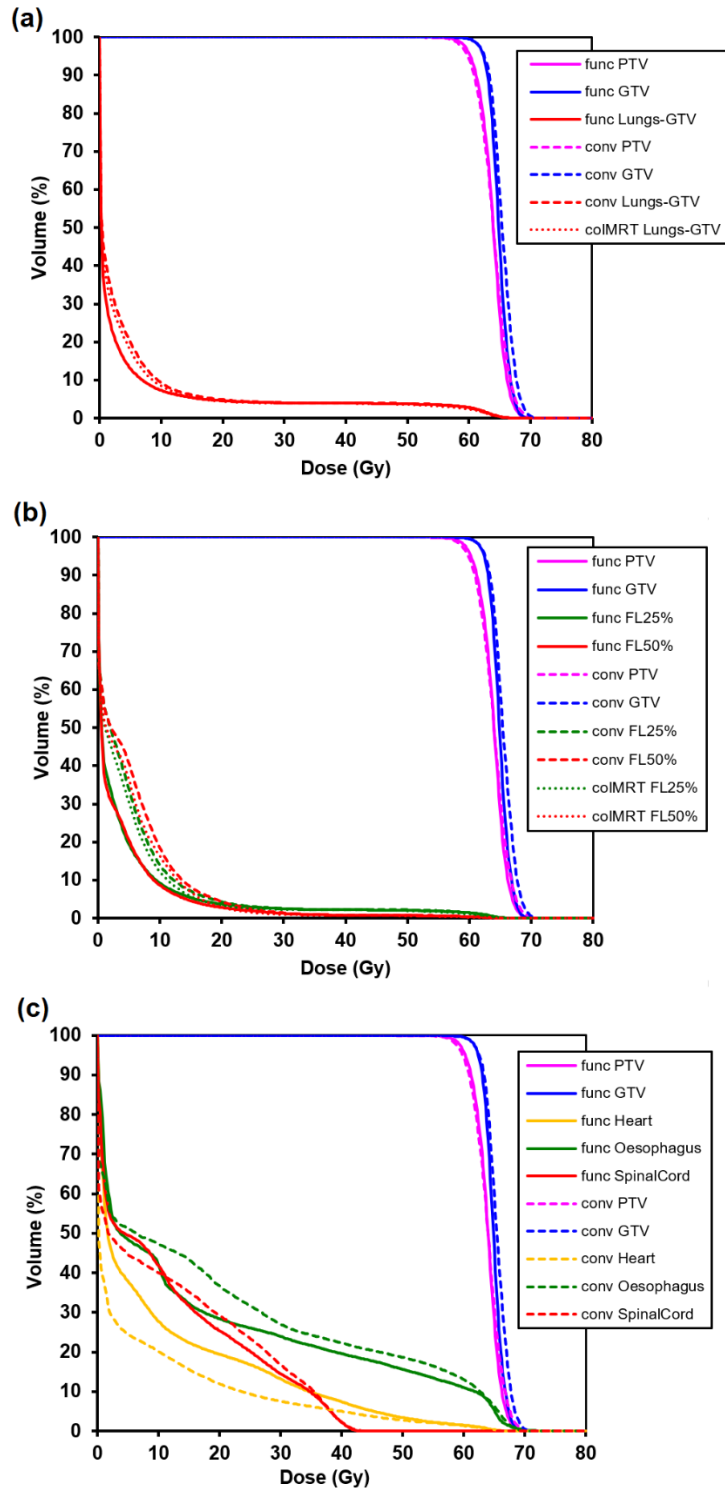
453

454

455

456

Figure 2. Beam orientation maps for the same patients as figure 1. The maps show the mean functionally weighted lung dose for a single beam at each combination of gantry and couch angle, for a 1Gy mean dose to the planning target volume. The dose in each map is displayed as a percentage of the maximum dose in the map. The grey regions are collision zones and the black points are the selected beam orientations. Note that the left- and right-hand edges of the graph represent the same beam orientations (gantry  $180^\circ$ ). Note also that gantry angle  $g$  at couch  $90^\circ$  is equivalent to gantry angle  $360^\circ - g$  at couch angle  $270^\circ$ . At gantry angle  $0^\circ$  and  $180^\circ$ , changing the couch angle merely changes the orientation of the collimator with respect to the PTV, so the vertical lines through gantry angles  $0^\circ$  and  $180^\circ$  are degenerate.



457

458

459

460

461

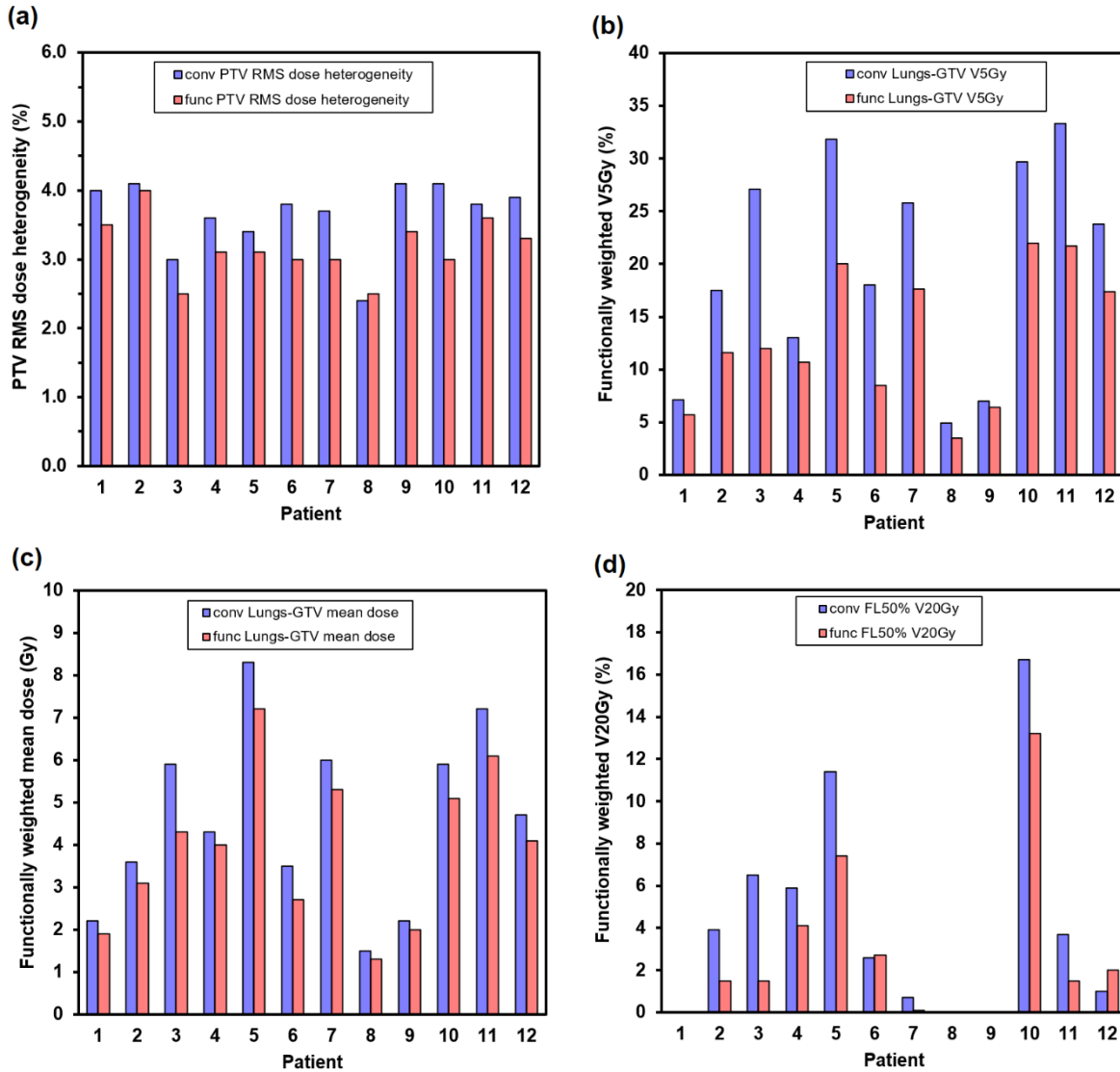
462

463

Figure 3. Mean dose-volume histograms for the functional (func) and conventional (conv) plans in the 12 patients. (a) Target volumes and whole lung, (b) target volumes and lung volume with at least 25% (FL<sub>25%</sub>) function and at least 50% (FL<sub>50%</sub>) function, (c) target volumes and normal structures. All of the lung dose-volume histograms show functionally weighted dose, whether conventionally or functionally planned. Parts (a) and (b) also show the dose-volume histograms for the coplanar IMRT comparison plan.

464

465



466

467

468

469

470

471

472

473

474

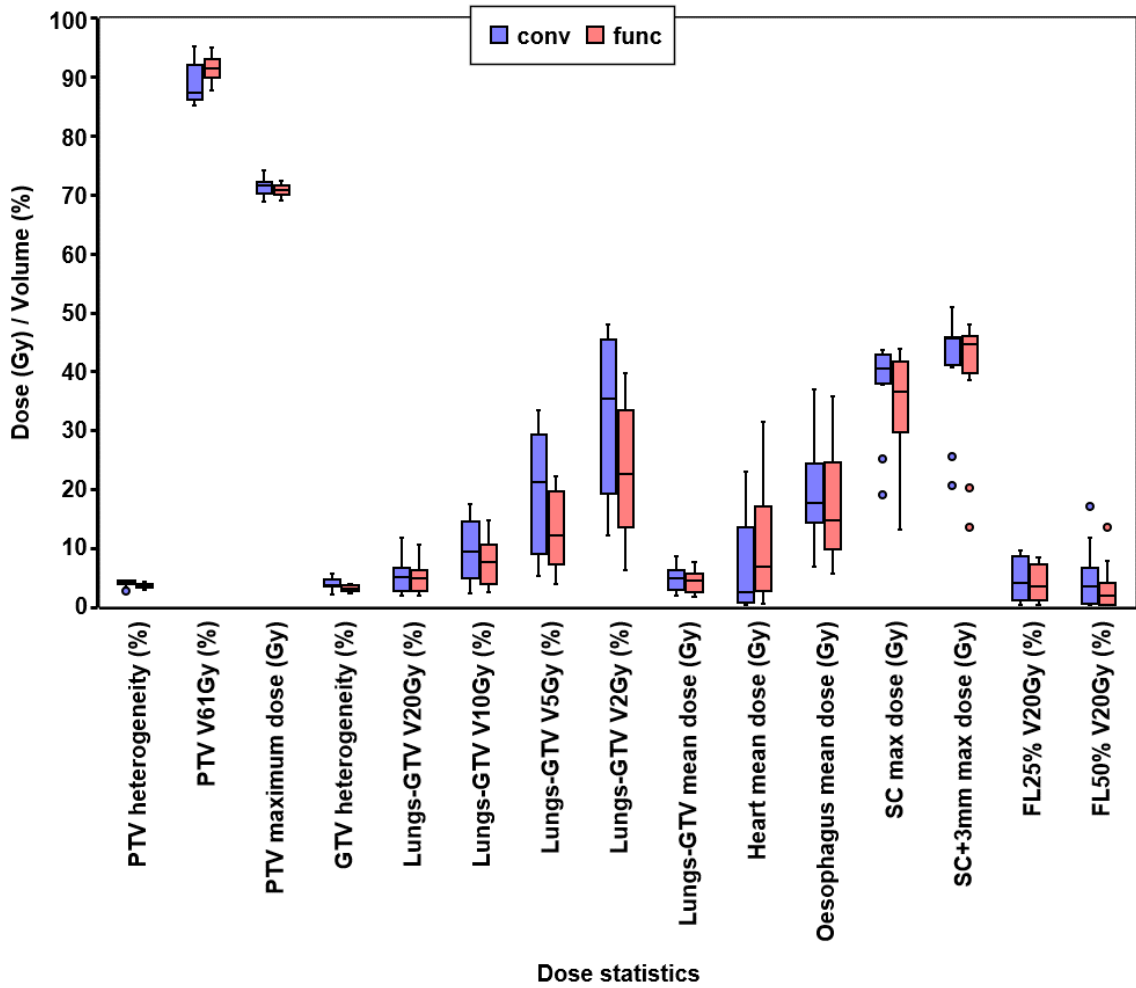
475

476

Figure 4. Comparison of conventional (conv) and functional (func) plans in the 12 patients. (a) Root mean square (RMS) dose heterogeneity with respect to 64Gy. (b) Functionally weighted V<sub>5Gy</sub>. (c) Functionally weighted mean lung dose. (d) Functionally weighted V<sub>20Gy</sub> for the lung with greater than 50% function (FL<sub>50%</sub>). In (d), V<sub>20Gy</sub> is shown, as opposed to V<sub>5Gy</sub>, as the function is higher in this region, so the functionally weighted dose is similar to the physical dose.

477

478



479

480

481

482

483

484

485

486

487

488

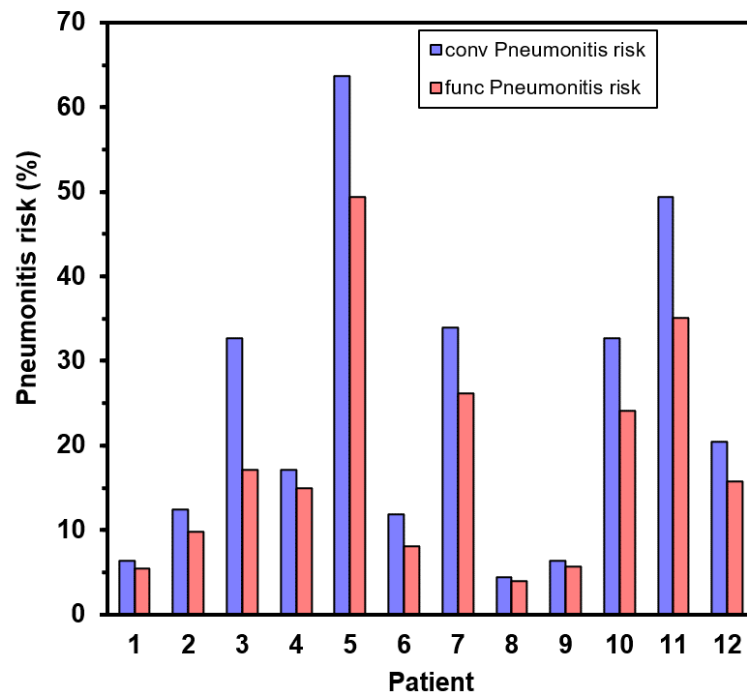
489

490

491

Figure 5. Comparison of key statistics for all structures for the conventional (conv) and functional (func) plans. The boxes show median and quartiles and the outliers are the points greater than 1.5 times the interquartile range from the quartile. PTV: planning target volume, GTV: gross tumour volume, SC: spinal cord, FL<sub>25%</sub>: lung with greater than 25% function, FL<sub>50%</sub>: lung with greater than 50% function. All statistics relating to lung (Lungs-GTV, FL<sub>25%</sub> and FL<sub>50%</sub>) are for functionally weighted dose and the remainder are for physical dose.

492



493

494

495

496 Figure 6. Comparison of predicted pneumonitis risk from the conventional (conv)

497 and functional (func) plans in the 12 patients according to the QUANTEC logistic model.

498

499